1 *Article*

2,3 Thiopurine Drugs Repositioned as Tyrosinase Inhibitors

4 **Joonhyuck Choi [1], You-Mie Lee [2] and Jun-Goo Jee [3,*]**

5 [1] Research Institute of Pharmaceutical Sciences, College of Pharmacy, Kyungpook National University,
6 80 Daehak-ro, Buk-gu, Daegu 41566, Republic of Korea; crowz124@naver.com
7 [2] Research Institute of Pharmaceutical Sciences, College of Pharmacy, Kyungpook National University,
8 80 Daehak-ro, Buk-gu, Daegu 41566, Republic of Korea; lym@knu.ac.kr
9 [3] Research Institute of Pharmaceutical Sciences, College of Pharmacy, Kyungpook National University,
10 80 Daehak-ro, Buk-gu, Daegu 41566, Republic of Korea; jjee@knu.ac.kr
11 * Correspondence: jjee@knu.ac.kr; Tel.: +82-53-880-7568

12 **Abstract:** In this study, we repositioned thiopurine drugs used for the treatment of acute
13 leukaemia as new tyrosinase inhibitors. Tyrosinase catalyses two distinct and successive
14 oxidations in melanin biosynthesis: the conversions of tyrosine to dihydroxyphenylalanine (DOPA)
15 and DOPA to dopaquinone. Continuous efforts are underway to discover small molecule
16 inhibitors of tyrosinase for therapeutic, cosmetic, and agricultural purposes. Structure-based
17 virtual screening has predicted inhibitor candidates for mushroom tyrosinase from drugs
18 approved by the US Food and Drug Administration (FDA). Enzyme assays have confirmed the
19 thiopurine leukaemia drug, thioguanine, as a tyrosinase inhibitor. Two other thiopurine drugs,
20 mercaptopurine and azathioprine, were also evaluated for their tyrosinase inhibitory activity;
21 mercaptopurine caused stronger inhibition than thioguanine did, whereas azathioprine was a
22 poor inhibitor. The inhibitory constants of thioguanine and mercaptopurine were calculated as
23 52 and 16 μM, respectively, and the value of mercaptopurine was comparable to that of the
24 well-known inhibitor kojic acid (13 μM). The cell lysate and melanin content assay in B16F10
25 melanoma cells confirmed that the compounds inhibited mammalian tyrosinase. In particular,
26 50 μM thioguanine reduced the melanin content by 57% without cytotoxicity. Furthermore,
27 the thiopurine drugs shared little chemical similarity with the known tyrosinase inhibitors.

28 **Keywords:** cheminformatics; docking simulation; drug repositioning; thiopurine; tyrosinase

29

30 1. Introduction

31   The colour of the human skin is predominantly determined by the amount of melanin
32 produced in the skin melanocytes. Dark-coloured eyes and hair, as well as browning of food, are
33 also related to elevated melanin content. The enzymatic reaction of tyrosinase is the primary
34 process in melanin production in living organisms. The cognate substrate, tyrosine, is converted
35 into dihydroxyphenylalanine (DOPA) and subsequently into dopaquinone by tyrosinase, and then
36 spontaneously into melanin via eumelanin. Tyrosinase, catechol oxidase, and haemocyanin are
37 type-3 copper proteins, which possess two juxtaposed copper ions in the catalytic centre. Three
38 evolutionarily conserved histidine residues form coordinate bonds with a copper ion. In the
39 hydroxylation of monophenol to diphenol and its subsequent conversion to quinone by tyrosinase,
40 catechol oxidase only catalyses the second oxidation. In contrast, the primary role of haemocyanin
41 in some invertebrates is the carriage of oxygen.
42   The copper ions of tyrosinase interchange among four oxidation states (oxy-, met-, deoxy-, and
43 deact-) [1]. The catalytic activity is coupled to the cycle, providing the substrates with molecular
44 oxygen. Quantum chemical calculations and spectroscopic studies of simplified chemical systems
45 have provided details of the catalytic cycle and copper states. Four atoms, two Cu(II)s and two
46 bridging oxygens, constitute the planar structure of the oxy-form. The oxidation states of the met-

47 and deoxy-forms are Cu(II)-Cu(II) and Cu(I)-Cu(I), respectively. The met-form, in which one or two
48 hydroxide molecules bridge two Cu(II)s, is assumed to be the resting state of tyrosinase. The
49 coordinate bonds between copper and histidine molecules are thought to be disrupted in the
50 deact-state.

51 The uncontrolled activity of tyrosinase causes disorders. For example, albinism is a congenital
52 disorder in which the body scarcely synthesises melanin owing to the absence of tyrosinase,
53 whereas overactivation of tyrosinase increases melanin synthesis, which causes skin problems.
54 Abnormalities in tyrosinase activity have also been associated with other diseases such as cancer
55 and Parkinson's disease [2-5]. Efforts to discover and develop small molecules that selectively
56 modulate the function of tyrosinase for the treatment of skin conditions have continued, including
57 the development of skin-lightening cosmetics and products for agricultural purposes [6-13].
58 Tyrosinase inhibitors can be largely divided into two classes: polyphenolic compounds and
59 thiourea derivatives [14]. The polyphenolic compounds are natural-based such as glycosylated
60 hydroquinones from plants and arbutin, a skin-lightening agent. Phenylthiourea and its analogues
61 constitute the other class.

62 The crystal structures of the complexes between two substrates, tyrosine and DOPA, and
63 bacterial tyrosinase show snapshot transition structures under conditions where zinc atoms replace
64 the copper atoms [15]. The structures revealed a subtle variation in the orientations of tyrosine and
65 DOPA, which facilitates the understanding of the differences in tyrosinase and catechol oxidase. In
66 contrast, the relevant complex structures with inhibitory effects are limited in number, which
67 makes it difficult to obtain a detailed explanation of tyrosinase inhibition. Three polyphenolic
68 compound complexes, one between tropolone and mushroom tyrosinase [16] and the other two
69 between kojic acid and hydroquinone and bacterial tyrosinase [17], are available. In addition, the
70 structures of complex formed between catechol oxidase and phenylthiourea has provided insight
71 into another type of inhibition [18]. These structures underscore that the binding of inhibitors to
72 tyrosinase does not result in the oxy-state but rather the met-state where the oxygen atoms of
73 tropolone, kojic acid, and hydroquinone, and the sulphur of phenylthiourea replace the bridging
74 oxygen atoms that exist in the apo-state.

75 Drug repositioning is defined as the application of the existing drugs to new uses.
76 Repositioning can reduce the time and cost required for the typical drug discovery process.
77 Accumulated pharmaceutical and toxicological data have uncovered the polypharmacological
78 networks of numerous drugs. Nevertheless, effective strategies for drug repositioning, particularly
79 those that are amenable to academic laboratories, are less well established. Computational methods
80 can significantly facilitate drug repositioning. We previously reported cheminformatics-based drug
81 repositioning, which resulted in the identification of ethionamide and its analogues [19] and
82 thiourea-containing drugs [20] as novel inhibitors of tyrosinase. In this study, we identified
83 additional agents for repositioning as new tyrosinase inhibitors using a structure-based virtual
84 screening (SBVS). Imperfections are present in the SBVS, exemplified by the improper handling of
85 protein flexibility and solvent molecules. Nevertheless, it has been successfully used in the drug
86 discovery process as a complementary strategy to high-throughput screening [21]. SBVS can enrich
87 the true-positives and decrease the number of test molecules to a manageable range using careful
88 assays. We have reported an optimised pairing of structures and software that led to the discovery
89 of new classes of potent tyrosinase inhibitors [22] and used the pairing for SBVS-based
90 repositioning.

91 ## 2. Results

92 ### *2.1. Structure-based docking simulation revealed thioguanine as a tyrosinase inhibitor*

93 In our previous study, the optimised pairing of an algorithm and three-dimensional (3D)
94 structures considerably improved the prioritisation of true-positives in the high-throughput virtual
95 screening of inhibitors of mushroom tyrosinase [22]. The reproduced poses of phenylthiourea and
96 tropolone were compared with those found in the crystal structures, leading to the selection of
97 DOCK 3.6 [23] as the docking algorithm among four software. Dockings with the molecular

98   dynamics simulation-derived ensemble using a mixture of known ligands and their
99   physicochemically matched but topologically different decoys led to the selection of the best
100 structure based on the metrics from the receiver operating characteristic (ROC) curve. We then
101 investigated whether the pair could facilitate drug repositioning. We used an identical pair of
102 algorithms and structures to screen a subset of the ZINC database [24-26], the US Food and Drug
103 Administration (FDA)-approved drugs (designated as DSSTOX) that comprises 3182 small
104 molecules. The top 10 compounds that showed the lowest energy were thioguanine
105 (ZINC18085533), tranilast (ZINC797), nifumic acid (ZINC125031), D-aspartic acid (ZINC895218),
106 S-carboxymethyl-L-cysteine (ZINC1529732), L-aspartic acid (ZINC895032), probenecid (ZINC1982),
107 diflunisal (ZINC20243), aminohippuric acid (ZINC119344), and etebenecid (ZINC1380) in
108 ascending order of their DOCK 3.6 energies (Figure 1). Interestingly, an extensive literature survey
109 found that the inhibition of tyrosinase by diflunisal and aminohippuric acid through direct binding
110 has been reported [27, 28]. However, there has been no report on whether the other eight molecules
111 inhibit tyrosinase. Therefore, we tested whether thioguanine, tranilast, nifumic acid, DL-aspartic
112 acid, S-carboxymethyl-L-cysteine, and probenecid could inhibit mushroom tyrosinase, but only
113 thioguanine exerted inhibitory action (Figure 2). The quantified inhibition expressed as the
114 inhibitory constant (K_i) was 52 µM (Table 1). It is noteworthy that the enzyme assay experiments
115 included 0.01% Triton X-100 to exclude false-positives caused by colloidal aggregation [29].
116 Considering the chemical similarity between probenecid and etebenecid, it would be reasonable to
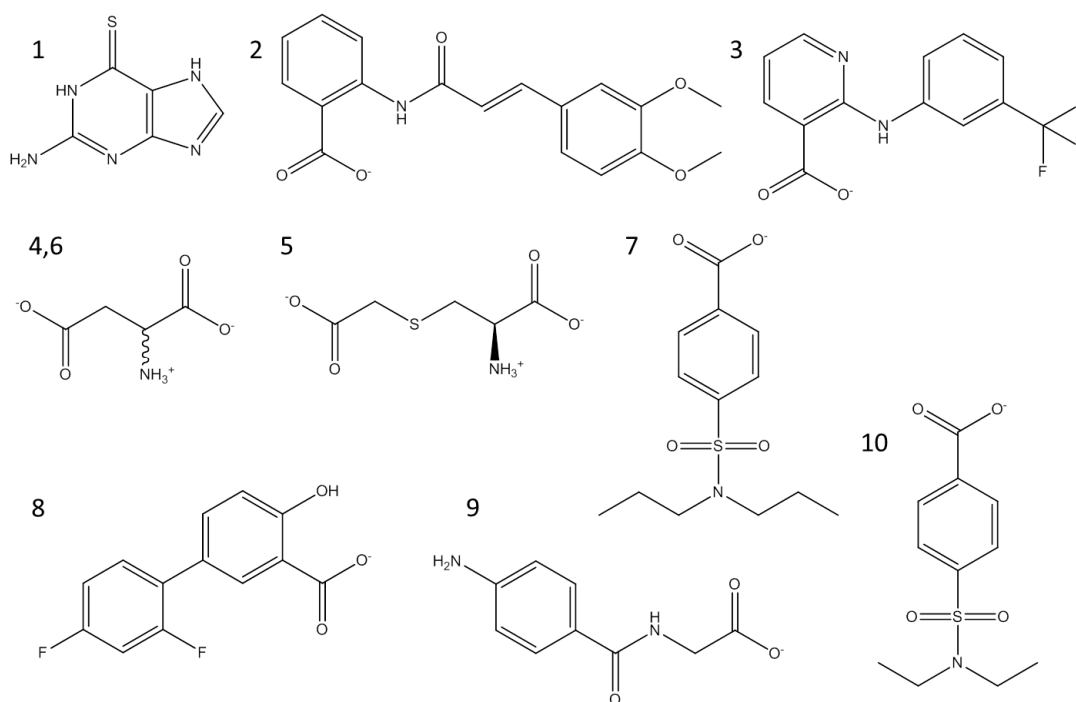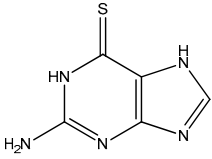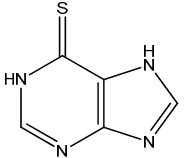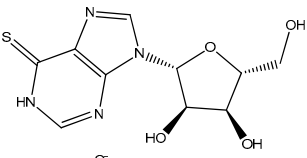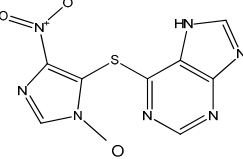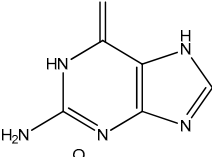117 assume that etebenecid also has no inhibitory effect.
118
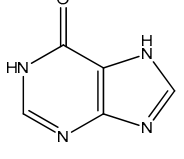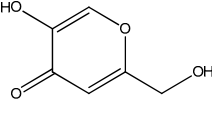
Figure 1. Top 10 candidate molecules predicted as potential tyrosinase inhibitors from the US Food and Drug Administration (FDA) subset of ZINC database. Molecules **1–10**, which showed the lowest DOCK 3.6 energies were thioguanine (ZINC18085533), tranilast (ZINC797), nifumic acid (ZINC125031), D-aspartic acid (ZINC895218), S-carboxymethyl-L-cysteine (ZINC1529732), L-aspartic acid (ZINC895032), probenecid (ZINC1982), diflunisal (ZINC20243), aminohippuric acid (ZINC119344), and etebenecid (ZINC1380).

119

Table 1. Details of compounds tested quantitatively for inhibition of mushroom tyrosinase

Chemical	2D structure	MW	LogP[&]	Ki (µM)	LE[#]
Thioguanine		167	0.60	52	0.49
Mercaptopurine		152	1.00	16	0.61
Thioinosine		284	-0.90	8	0.34
Azathioprine		277	1.15	>1000	NA
Guanine		151	-0.77	>1000	NA
Hypoxanthine		136	-0.35	>1000	NA
Kojic acid		142	-0.16	13	Control

[&] LogP values were extracted from the ZINC database [24-26].

[#] LE, ligand efficiency is defined as $-1.37 \times (\mathrm{Log}_{10}K_i)/HA$, where HA indicates the number of heavy atoms [44].

120

2.2. Mercaptopurine and thioinosine inhibited tyrosine activity

122 Thioguanine, also called tioguanine or 6-thioguanine, is a drug for the treatment of leukaemia.
123 It is one of the essential medicines that the World Health Organization specifies are required for a
124 basic health system. In addition to thioguanine, mercaptopurine (ZINC4658290) and azathioprine
125 (ZINC4258316) comprise the thiopurine family of drugs. However, in contrast to thioguanine and
126 mercaptopurine, immunosuppression is the primary indication of azathioprine. We evaluated
127 whether mercaptopurine and azathioprine inhibit tyrosinase and found that mercaptopurine but
128 not azathioprine exerted an inhibitory activity (K_i = 16 µM, Figure 2). This suggests that the sulphur
129 atom possibly plays a significant role in the interaction with tyrosinase. To confirm this hypothesis,
130 we conducted enzymatic assays with guanine (ZINC895129), hypoxanthine (ZINC36378435), and
131 thioinosine (also known as mercaptopurine-riboside, ZINC4217548). Guanine and hypoxanthine are
132 analogues of thioguanine and mercaptopurine, respectively, in which oxygen atoms replace
133 sulphur atoms. The metabolism of mercaptopurine generates thioinosine in humans through the
134 attachment of sugar at the opposite position to that of sulphur in purine. Of these molecules, only

135   thioinosine inhibited tyrosinase (K_i = 8 µM, Figure 2). These results were consistent with our
136   previous data that emphasised the importance of sulphur in ethionamide and thiourea-containing
137   drugs for the inhibition of tyrosinase [19, 20]. The quantified value of the tyrosinase inhibition by
138   mercaptopurine was comparable to that of kojic acid (13 µM), a well-known and potent tyrosinase
139   inhibitor, under the same experimental conditions (Table 1). We measured the change in T_m value
140   using differential scanning fluorimetry (DSF) to confirm direct binding. An increase or decrease in
141   the T_m value reflects the stabilisation or destabilisation of a protein following direct binding with
142   inhibitors, respectively. DSF showed there was a shift in the T_m values of tyrosinase from 51.8°C to
143   49.8, 49.0, and 51.0 °C in the complexes with thioguanine, mercaptopurine, and thioinosine,
144   respectively (Figure 3). The degrees of change (ΔT_m) in the three inhibitors were all statistically
145   significant ($p < 0.01$). A decrease in this value is indicative of the destabilisation of the protein
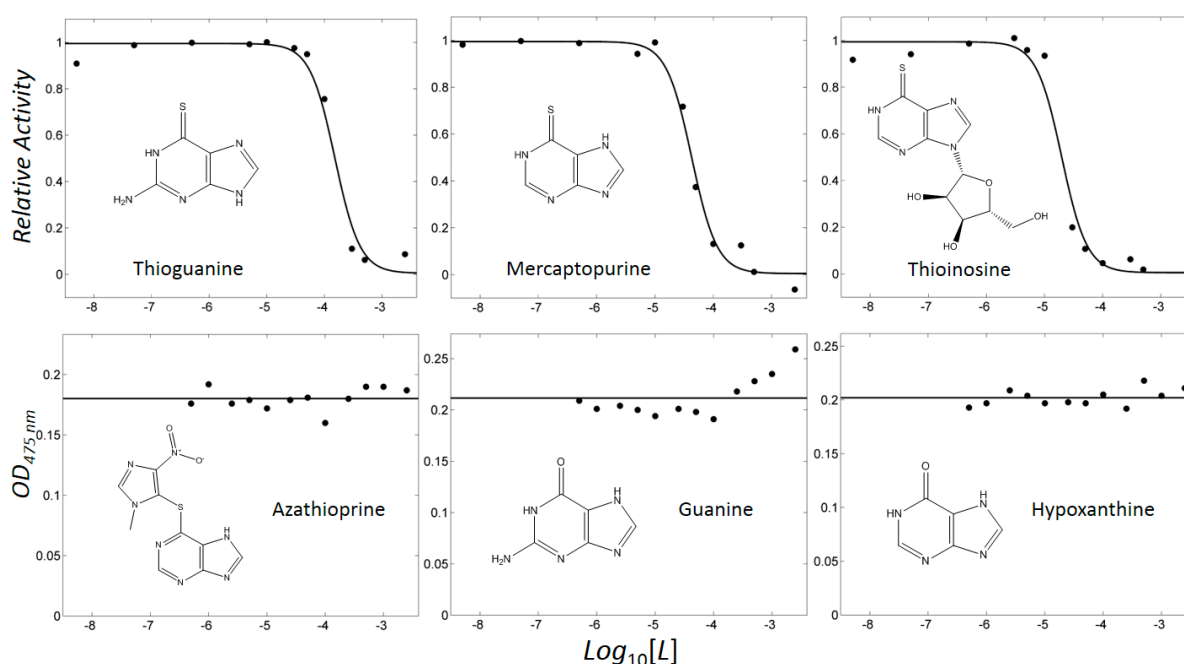146   following its direct binding with the inhibitors.

147

Figure 2. Profiles showing concentration-dependent inhibition. Activities were scaled to a relative value in the range of 0–1 for thioguanine, mercaptopurine, and thioinosine. Optical densities at 475 nm (OD_{475nm}) were shown for azathioprine, guanine, and hypoxanthine.

148

149   *2.3. Enzyme inhibitory kinetics classified thiopurine drugs as competitive inhibitors*
150   The kinetics of enzymes with inhibitory action classified thioguanine, mercaptopurine, and
151   thioinosine as competitive inhibitors. We directly fitted all substrate and inhibitor
152   concentration-dependent velocities using the modified Michaelis–Menten equation in a nonlinear
153   manner through the minimisation of χ^2 values in four kinetic models: competitive, uncompetitive,
154   non-competitive, and mixed [30, 31] (Figure 4). Among the competitive, uncompetitive, and
155   non-competitive models, the competitive model showed the smallest values for the three
156   compounds. The values of reduced χ^2, χ^2 divided by the degree of freedom for thioguanine,
157   mercaptopurine, and thioinosine in the competitive model were 0.08, 0.91, and 0.43, respectively.
158   The F-test showed that no statistical significance occurred in the mixed model compared to the
159   competitive model. The assigned models were sound considering that the three molecules share
160   functional moieties. The qualitative agreement of the experimental and fitted inhibitory constant, K_i,
161   also supported the soundness of the analyses. The kinetically fitted K_i values for thioguanine,
162   mercaptopurine, and thioinosine were 40, 29, and 14 µM, respectively. It is noteworthy that in this
163   situation, the apparent kinetics was observed. The underlying mechanism would be more
164   complicated, and the limited precision of the current dataset would make it difficult to extract the
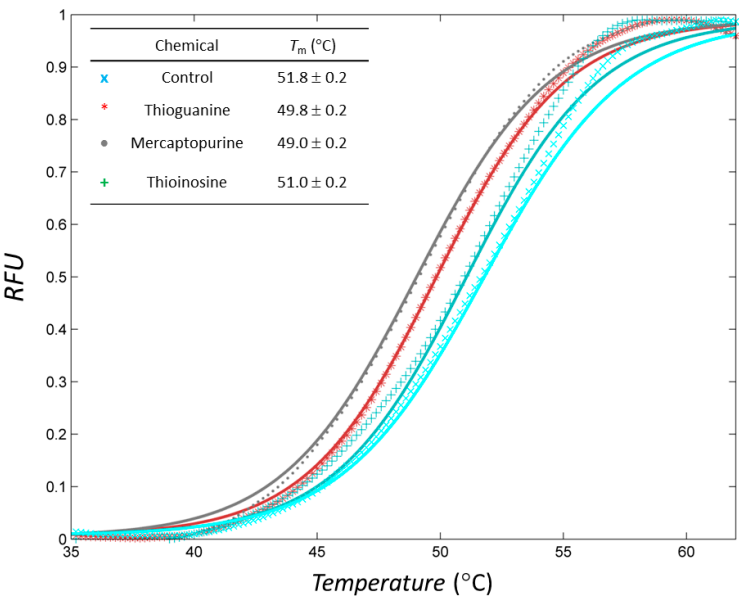165   details [32].

166

Figure 3. Profiles of differential scanning fluorimetry (DSF) analyses of inhibitors. Markers and lines indicate the raw and fitted data, respectively, in each case. Normalised profiles with relative fluorescence unit (RFU) were constructed in the range of 35–65 °C.

167
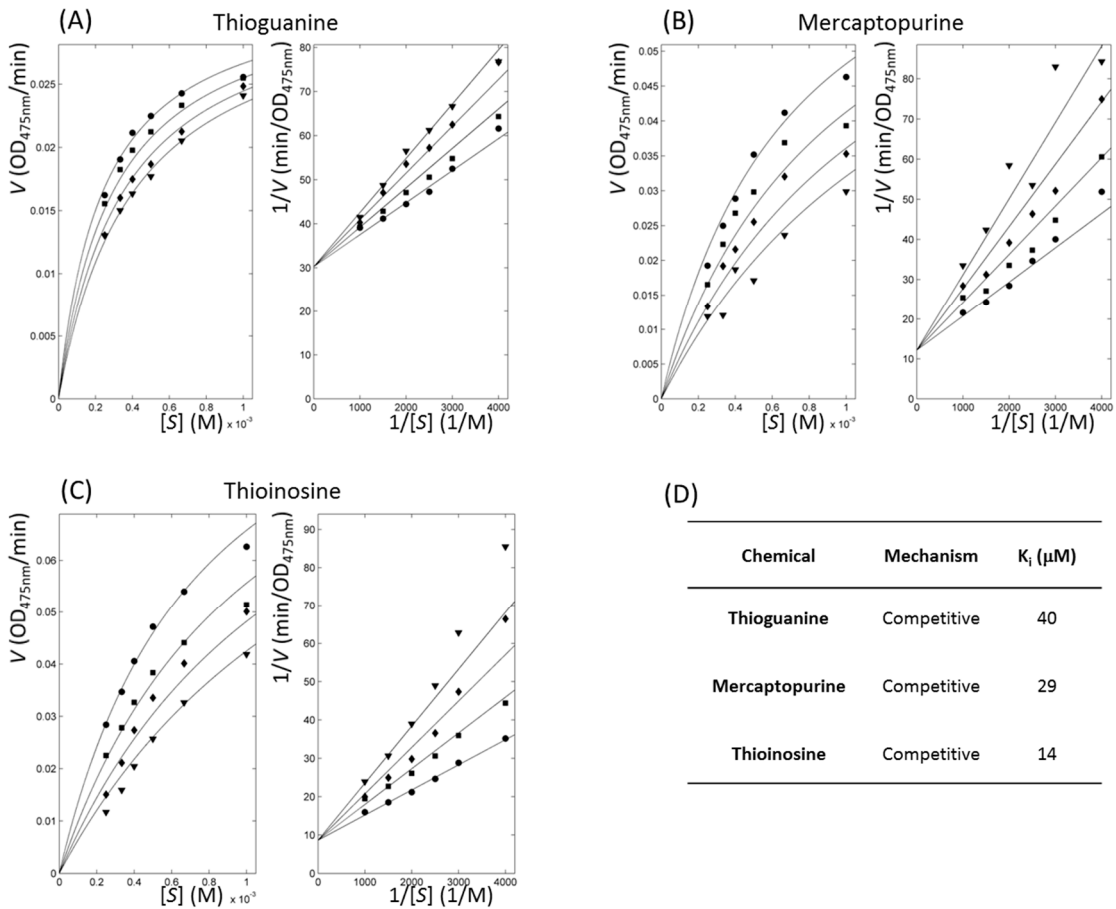
Figure 4. Inhibitory enzyme kinetics with tyrosinase inhibitors. (A–C) Left and right panels show Michaelis–Menten and Lineweaver–Burk plots, respectively for each labelled compound. Respective symbols, ●, ■, ♦, and ▼ represent inhibitor profiles at concentrations of 90, 120, 150, and 180 μM for thioguanine; 20, 40, 60, and 80 μM for mercaptopurine; and 10, 20, 30, and 40 μM for thioinosine. (D) Parameters of enzyme inhibitory kinetics are listed. K_i indicates fitted dissociation constants of the protein-inhibitor complex using nonlinear

data fitting, assuming a competitive model.

2.4. Thiopurine drugs also inhibited mammalian tyrosinase

To determine whether the thiopurine-drugs inhibit mammalian tyrosinase, we performed an enzymatic assay with melanoma B16F10 cell lysates. The addition of thioguanine, mercaptopurine, and thioinosine to the lysates inhibited melanin syntheses in a concentration-dependent manner. Mercaptopurine exhibited the highest inhibition, showing a comparable decrement to that induced by kojic acid (Figure 5). The cytotoxicity and the cellular activity of thioguanine, mercaptopurine, and thioinosine were assessed using the 3-(4,5-dimethylthiazol-2-yl)-2,5-diphenyltetrazolium bromide (MTT) and melanin content assays, respectively, in B16F10 cells. The addition of up to 50 μM of any of the three inhibitors did not notably decrease the reduction in the MTT reaction under these experimental conditions. Thioguanine and thioinosine markedly reduced the melanin content at 20 and 50 μM (Figure 5). In particular, the quantification of the decrease caused by 50 μM thioguanine showed it was approximately 57%. The decrement was considerably more than that exerted by kojic acid and comparable with that of phenylthiourea [19, 20]. In addition to the structural differences that were dependent on living species, other factors associated with the polypharmacology and pharmaceutics may have led to the inconsistencies observed between the enzyme-based and melanin content assays.
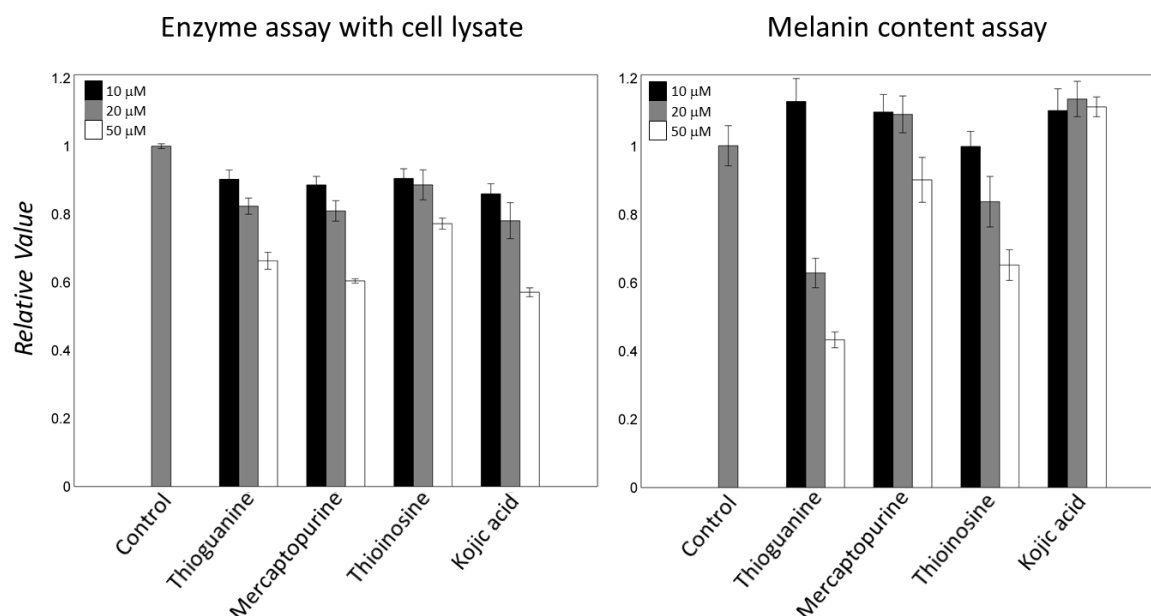

Figure 5. Mammalian tyrosinase inhibition. B16F10 cell lysates were used to evaluate inhibition against different concentrations of mammalian tyrosinase inhibitors. Melanin contents were measured at concentrations that exerted only a small effect on cell growth of B16F10 cells. Data are expressed as relative values to those of untreated control cells. Error bars indicate standard deviations of three repeated experiments per each condition.

2.5. Docking simulation suggested intermolecular interactions involved atomic contributions

In the modelled structures, the thiopurine moieties of thioguanine, mercaptopurine, and thioinosine almost completely overlapped (Figure 6). Of the four inhibitors (tropolone, kojic acid, hydroquinone, and phenylthiourea) reported to form complex structures with tyrosinase or catechol oxidase, phenylthiourea possessed a similar functional moiety to that of current inhibitors [16-18]. The limited sequence identity between mushroom tyrosinase and catechol oxidase (< 20%) makes the direct interpretation of the binding mode of phenylthiourea to mushroom tyrosinase equivocal. Nonetheless, it can be assumed that the position of the functional moiety does not change between the two structures. The sulphur atom of the thiopurine moiety lies at an almost identical position to that of phenylthiourea, bridging two copper atoms. The distances between the

197 two copper atoms and the sulphur of phenylthiourea in the crystal structures were 2.26 and 2.33 Å,
198 and those in the docked thioguanine were 2.50 and 2.56 Å, reflecting the similarity of the two
199 bound poses (Figure 6). However, a difference also exists between the structure of the
200 phenylthiourea-catechol oxidase complex and the docked models of thiopurine-tyrosinase. While
201 the nitrogen between the thione and phenyl groups of phenylthiourea is in contact with a copper
202 atom in the crystal structure [18], the very next nitrogen to the thione group of thiopurine forms an
203 intermolecular hydrogen bond with the $O\varepsilon 1/2$ of Glu-256 in the models (Figure 6). The discrepancy
204 may be attributed to the imperfections in the docking algorithm or the difference in the protein and
205 inhibitor. New 3D structures of tyrosinase in complex with inhibitors would be necessary to
206 provide an unambiguous explanation. In thioinosine, additional contacts with the side-chains of
207 Asn-260, Phe-264, and Val-283 were observed, which was thought to have caused the stronger
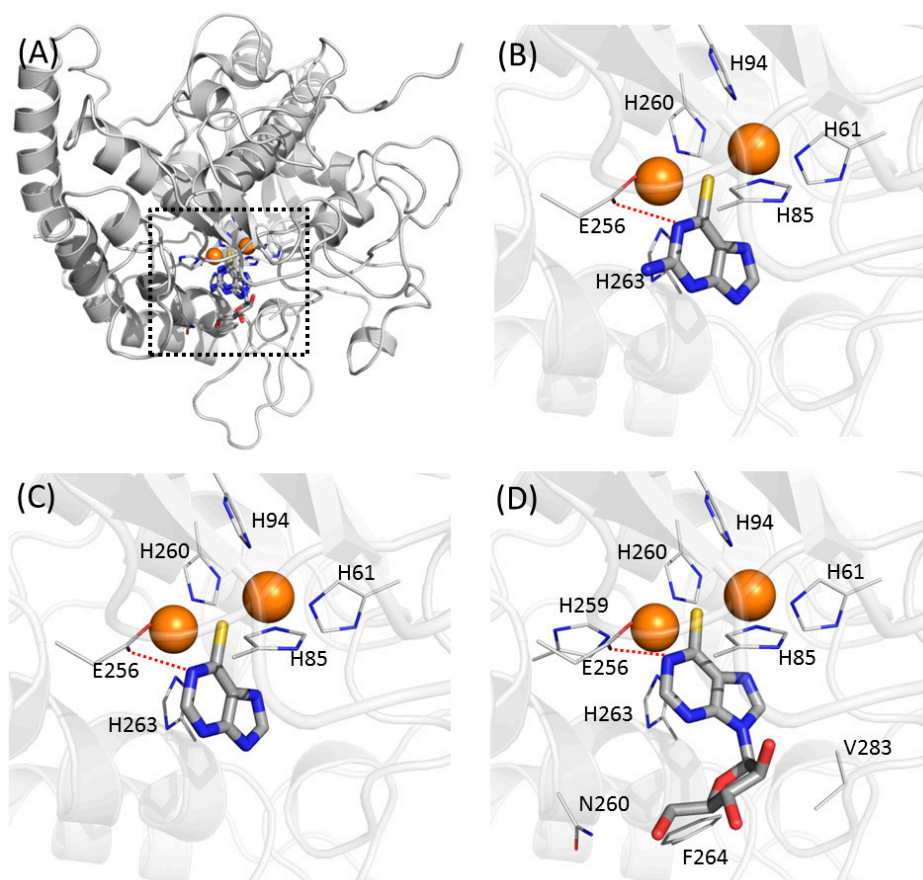208 inhibition.
209

Figure 6. Predicted binding modes of thiopurine inhibitors in this study. (A) Overlaid poses against mushroom tyrosinase. Two copper atoms in tyrosinase are indicated as orange spheres. Predicted binding modes in (B) thioguanine, (C) mercaptopurine, and (D) thioinosine are represented. Residues involved in intermolecular contacts from tyrosinase are labelled. Lines indicate intermolecular hydrophilic interaction. Figures were prepared and arranged to have identical direction using Pymol [51].

210
211 ***2.6. Cheminformatics supported novel chemical structures in thiopurine tyrosinase inhibitors***
212   We searched the chemically similar known inhibitors. BindingDB (2015m6 version) [33]
213 contains 486 small molecules that inhibit tyrosinase through direct binding from all species. Among
214 the molecules, the most similar inhibitor to thioguanine and mercaptopurine was
215 4-amino-5-(4-pyridyl)-4H-1,2,4-triazole-3-thiol (ZINC509439), with Tanimoto coefficient (Tc) values
216 of 0.15 and 0.18, respectively (Figure 7A). The reported K_i value of the compound was 1 μM. In
217 contrast, 4-(β-D-allopyranosyloxy)benzaldehyde (ZINC5234422) showed the closest similarity to
218 thioinosine, with a Tc value of 0.27 and a half-maximal inhibitory concentration (IC_{50}) of 94 μM. The

219   smaller Tc value indicated that the thiopurine drugs showed limited chemical similarities to the
220   known inhibitors, which was supported by the apparent differences. To assess the limited similarity
221   in detail, we used the similarity ensemble approach (SEA) [34], which involves summing up the Tc
222   values between a test molecule and a set of small molecules to obtain the ΣTc. The histogram of the
223   ΣTc values between a set of inhibitors shows the distribution of chemical similarities. Comparing the
224   ΣTc value of a test molecule and the distribution can demonstrate the chemical novelty of a test
225   molecule. A molecule that has greater chemical similarity to the others would exhibit a higher ΣTc
226   value. The ΣTc values were 27.62, 26.45, and 39.95 for thioguanine, mercaptopurine, and thioinosine,
227   respectively (Figure 7B). The values were ranked as number 480, 482 and 467 of the 486 tyrosinase
228   inhibitors from the highest score molecule, ZINC28645001, which is a 2,4-resorcinol derivative and
229   has a ΣTc value of 93.87 [35]. Owing to the central roles and frequent use of DNA bases in living
230   organisms and its close similarity to guanine, thioguanine has been reported as a direct binder of
231   various cellular proteins. A literature search of the ChEMBL database [36] revealed that thioguanine
232   (ID: CHEMBL727) inhibited the functions of p21 (RAC1) activated kinase 1 (PAK1) [37],
233   6-oxopurine phosphoribosyltransferases [38], human xanthine oxidase [39], uridine nucleoside
234   ribohydrolase [40], and monoamine oxidase (MAO)-A,B [41] through direct binding. As purine is
235   the core moiety responsible for the effects of these proteins, both guanine and thioguanine are
236   inhibitory. Indoleamine 2,3-dioxygenase 1 is one of the known targets of mercaptopurine
237   (CHEMBL1425) and is a protein that is inhibited by thioguanine [42]. A previous study reported the
238   interaction between thioinosine (CHEMBL448290) and MAO-A/B [41]. However, to the best of our
239   knowledge, no known target proteins related to skin pigmentation have been reported.
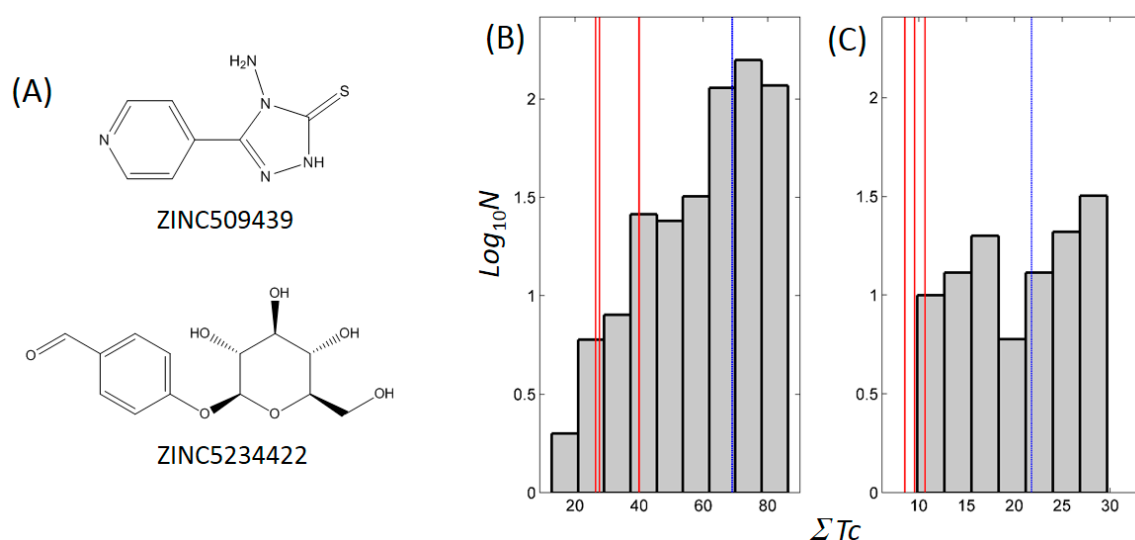240

Figure 7. Quantification of chemical similarity to known tyrosinase inhibitors. (A) Of the 418 BindingDB-deposited known inhibitors [33], the most similar ones to the inhibitors in this study are presented. ZINC509439 showed the closest chemical structure to thioguanine and mercaptopurine with Tanimoto coefficients (Tc) of 0.15 and 0.18, respectively, whereas the closest inhibitor to thioinosine was ZINC509439 with a Tc of 0.27. Histograms of distributions of ΣTc values of (B) all and (C) 115 thione-containing tyrosinase inhibitors are presented. ΣTc is defined as the sum of Tcs between a test molecule and a set of inhibitors. *N* in y-axes means the frequency. ΣTc values of thioguanine, mercaptopurine, and thioinosine were (B) 27.62, 26.45, and 39.95 and (C) 9.58, 8.56, and 10.68, respectively. Corresponding positions are shown as red lines. Mean ΣTc values in all and 115 thione-containing tyrosinase inhibitors were 69.00 and 21.81, respectively, and denoted as dashed blue lines.

241

3. Discussion

243   Several cases of drug repositioning used SBVS [43], which is primarily targeted at discovering
244   inhibitors of new chemotypes, which cannot be identified using quantitative structure-activity

245 relationship analyses. The limited similarity to the known inhibitors may hinder the repositioning
246 of thiopurine drugs as tyrosinase inhibitors using cheminformatic methods. Even in SBVS, a
247 conventional approach, was insufficient for the repositioning of thioguanine. The use of the
248 optimised pair of structure and algorithm was indispensable. Specifically, the six coordinates from
249 the two crystal structures of mushroom tyrosinase (2Y9W and 2Y9X) [16] generated different
250 candidates, even with the same protocol and database. In the structures of 2Y9W-A (PDB ID-Chain),
251 2Y9W-B, 2Y9X-A, 2Y9X-B, 2Y9X-C, and 2Y9X-D, the rankings of docked thioguanine were 11, 13, 24,
252 21, 25, and 17, respectively. Although we cannot exclude the possibility that the highly ranked
253 candidates are inhibitory as well, the results clearly demonstrate the dependence of the scoring
254 function in SBVS on the template structure and the need to select the best structure and docking
255 algorithm pair. It should be noted, that software programs other than DOCK 3.6, AutoDock,
256 AutoDock Vina, and DOCK 6.7, were unsuccessful in generating the poses of tropolone or
257 phenylthiourea observed in X-ray structures in our previous study [22].

258   The inhibitory effects of the compounds against tyrosinase may not be deemed as strong.
259 However, it is noteworthy that mercaptopurine had a ligand efficiency (LE) value of 0.61 (Table 1).
260 In the drug discovery process, an LE value > 0.4 is a good criterion for determining the feasibility of
261 further developing a hit into a lead compound [44]. The LE values of thioguanine and thioinosine
262 were 0.49 and 0.34, respectively. The stronger inhibition induced by mercaptopurine than by
263 thioguanine is difficult to explain using the current docking models because both molecules have
264 almost identical binding poses. One possible explanation is the steric hindrance that could arise
265 from the amide group in thioguanine. The different electrostatic charges around the metal binding
266 region may be responsible for the difference.

267   The small molecule inhibitors of metalloenzymes generally possess a metal-binding group that
268 forms the coordinate bonds with catalytic metal cofactors. Our previous experiments classified the
269 metal-binding motifs in tyrosinase inhibitors into four types: carboxylate, thione, triazole, and
270 tetrazole [22]. In addition, some polyphenol compounds can inhibit tyrosinase by mimicking the
271 substrate. In the current study, thioguanine was included in the thione group. The other molecules
272 in the 10 candidate drugs identified by SBVS included carboxylates. Nevertheless, the six tested
273 molecules hardly inhibited mushroom tyrosinase, which indicates that the existence of the
274 metal-binding group is not only a sufficient but also a necessary condition. The cheminformatics
275 analysis revealed that 115 molecules of BindingDB-derived 486 inhibitors contain a thione moiety.
276 With the exception of the molecules with polyphenol moieties, only two (ZINC1706841 and
277 ZINC2019878) possess thiones to which no nitrogen is bound. Both are xanthate molecules [45], and
278 it is noteworthy that xanthate is a typical metal chelator. All other thione-containing
279 non-polyphenol inhibitors contain a nitrogen that can be used for the intermolecular electrostatic
280 contact. However, the thiopurine inhibitors in the current study showed little similarity to other
281 thione-containing tyrosinase inhibitors. The ΣTc values against the 115 thione-containing molecules
282 were 9.58, 8.56, and 10.68 for thioguanine, mercaptopurine, and thioinosine, respectively (Figure
283 7C). No inhibitor showed a smaller ΣTc than that of thioguanine and mercaptopurine, whereas
284 thioinosine was ranked as number 113.

285   In conclusion, we demonstrated an SBVS-based drug repositioning strategy where the
286 sophisticated combination of the docking algorithm and the template structure successfully
287 enriched the inhibitory compounds. Enzyme- and cell-based assays were used to confirm the
288 prediction. Our approach represents an extremely useful addition to drug repositioning methods
289 by using computational tools. Moreover, new inhibitors and their proposed inhibitory mechanisms
290 in this study will be valuable information for the development of more potent and selective
291 inhibitors of metalloenzymes.

292

4. Materials and Methods

294   Structure-based virtual screening — An in-house script, Automated pLatform for Integrative
295 Structure-based DOCKing (ALIS-DOCK), was prepared and used to perform the SBVS with the

296 molecules from a subset of ZINC database named "FDA-approved drugs (via DSSTOX)" [26]. For
297 the docking engine, ALIS-DOCK used DOCK 3.6 [23]. ALIS-DOCK used the structure chosen for
298 the structure-based high-throughput virtual screening as a template. The protocol for docking was
299 identical in principle to that of DOCK Blaster [46]. Molecules in the flexibase format with ligand
300 desolvation scoring terms [23] were directly adapted from the ZINC database [26]. The scoring
301 function of DOCK 3.6 is the sum of the van der Waals and electrostatic energies corrected by the
302 desolvation terms. The charge for copper atoms was reduced from 1.40 to 0.73, based on the
303 quantum chemical calculations [22].
304   Cheminformatics — The Tc was used to quantify the similarity between two small molecules.
305 The Morgan circular fingerprints implemented in RDKit (http://www.rdkit.org) digitise the
306 functional moieties in a molecule. Tc evaluates the common over the union digitised features
307 between two molecules and is a value between 0 and 1. Two chemicals sharing no and complete
308 overlap show Tc values of 0 and 1, respectively. Inhibitors of tyrosinase from all species were
309 extracted from the BindingDB database [33]. The in-house script, Automated LIgand Search for
310 PolyPharmacology (ALIS-PP) was used to automate the cheminformatics procedure.
311   Enzyme activity and kinetics experiments with inhibitors — All reagents used in this study
312 were purchased from ChemBridge (San Diego, CA, USA), Sigma-Aldrich (St. Louis, MO, USA), or
313 Tokyo Chemical Industry (Tokyo, Japan). The reaction solution for the enzyme assay was prepared
314 with 200 nM mushroom tyrosinase and inhibitors in phosphate-buffered saline (PBS) containing 5%
315 dimethyl sulphoxide and 0.01 % (w/v) Triton X-100. After incubating the mixture at 30°C for 10 min,
316 500 μM L-tyrosine was added as the substrate. Subsequently, the absorbance change induced by the
317 chromogenic product, dopachrome, was measured at 475 nm. The IC_{50} was evaluated by analysing
318 different concentrations of each inhibitor. The inhibitory constants (K_i) were converted from the IC_{50}
319 values using the K_m obtained from kinetics experiments and substrate concentration based on the
320 Cheng–Prusoff equation [47]. A series of substrates at concentrations of 0.25, 0.33, 0.4, 0.5, 0.67, and
321 1 mM were used to obtain the respective velocities (V) for enzyme inhibitory kinetics. The
322 concentrations of each inhibitor were varied and comprised the range that included the IC_{50} value.
323 Four models (competitive, uncompetitive, non-competitive, and mixed) derived from the
324 Michaelis–Menten equation were used [48] to fit the kinetic parameters, maximum velocity (V_{max}),
325 Michaelis constant (K_m), and the dissociation constants between the substrate-free enzyme and
326 inhibitor (K_{ic}) and the substrate-bound enzyme and inhibitor (K_{iu}). The data from all concentrations
327 of the substrate and inhibitor were simultaneously fitted nonlinearly by minimising the χ^2 value,
328 defined as the sum of the squared deviations between experimental and fitted values [30] for each
329 model. The appropriate model was selected based on the F-test with χ^2 values from the four models,
330 coupled with the extraction of the related parameters [30, 49]. All fittings and statistical analyses in
331 this study were computed by using MATLAB® (MathWorks, Natick, MA, USA).
332   DSF — The stability of mushroom tyrosinase in the presence and absence of inhibitors was
333 assessed using DSF using a reverse transcription-polymerase chain reaction (RT-PCR) CFX96
334 system (BioRad, Hercules, CA, USA). After the addition of 5× SYPRO Orange to the solutions of 0.5
335 μM protein without or with 200 μM inhibitor, the temperature was gradually increased from 30 to
336 90°C to excite the dye at 492 nm, and the intensity of the emitted fluorescence was measured at 610
337 nm. The T_m value, which is the mid-point melting temperature, was calculated from a nonlinear fit
338 of the temperature-dependent fluorescent intensity $I(T)$, expressed as the Boltzmann equation:

339
$$I(T) = LL + \frac{UL - LL}{1 + \exp(\frac{T_m - T}{a})},$$

340 where *UL* and *LL* are related to the baseline and top of the curves, respectively, and *a* is the
341 steepness of the slope [50]. Only data in the range of 35–65°C were used for the fitting.
342   Cell-based activity assays with inhibitors — The melanin content and MTT conversion were
343 measured in B16F10 murine melanoma cells purchased from the Korean Cell Line Bank (Seoul,
344 Korea). When the density of B16F10 cells reached 1×10^5 cells, the test inhibitors (10, 20, and 50 μM)
345 and 3-isobutyl-1-methylxanthine (IBMX, 100 μM) were added, and the cells were incubated for 48 h.

346   The amount of melanin released into the extracellular area was quantified by measuring the
347   absorbance at 405 nm and was subsequently expressed as a percentage relative to the untreated
348   control. The change in the reduction of the MTT dye into formazan in the cell was quantitatively
349   interpreted as the cellular toxicity induced by the inhibitor. The inhibition of tyrosinase was also
350   estimated using the B16F10 cell lysates, as described previously [19]. In brief, the cells were lysed in
351   PBS supplemented with 1% (w/v) Triton X-100, centrifuged at 14,000 *g* for 30 min, and then the
352   supernatants were dialysed to remove Triton X-100. After adding 500 µM L-DOPA and the
353   inhibitors (10, 20, and 50 µM) to the prepared lysates, the change in absorbance over time at 475 nm
354   was measured. The decrease in absorbance was calculated relative to the absorbance of the
355   untreated controls.

358   **Author Contributions:** J.-G.J. designed the research project and wrote the manuscript. J.C. and J.-G.J. carried
359   out the experiments. All the authors analysed the data and proofread the manuscript.

360   **Conflicts of Interest:** The authors declare no conflict of interest.

References

362   1.   Ramsden, C. A.; Riley, P. A., Tyrosinase: the four oxidation states of the active site and their relevance
363   to enzymatic activation, oxidation and inactivation. *Bioorg Med Chem* **2014**, 22, 2388-95.
364   2.   Cavalieri, E. L.; Li, K. M.; Balu, N.; Saeed, M.; Devanesan, P.; Higginbotham, S.; Zhao, J.; Gross, M. L.;
365   Rogan, E. G., Catechol ortho-quinones: the electrophilic compounds that form depurinating DNA
366   adducts and could initiate cancer and other diseases. *Carcinogenesis* **2002**, 23, 1071-7.
367   3.   Asanuma, M.; Miyazaki, I.; Ogawa, N., Dopamine- or L-DOPA-induced neurotoxicity: the role of
368   dopamine quinone formation and tyrosinase in a model of Parkinson's disease. *Neurotox Res* **2003**, 5,
369   165-76.
370   4.   Pan, T.; Li, X.; Jankovic, J., The association between Parkinson's disease and melanoma. *Int J Cancer*
371   **2011**, 128, 2251-60.
372   5.   Sendoel, A.; Kohler, I.; Fellmann, C.; Lowe, S. W.; Hengartner, M. O., HIF-1 antagonizes p53-mediated
373   apoptosis through a secreted neuronal tyrosinase. *Nature* **2010**, 465, 577-83.
374   6.   Chang, T. S., An updated review of tyrosinase inhibitors. *Int J Mol Sci* **2009**, 10, 2440-75.
375   7.   Loizzo, M. R.; Tundis, R.; Menichini, F., Natural and Synthetic Tyrosinase Inhibitors as Antibrowning
376   Agents: An Update. *Comprehensive Reviews in Food Science and Food Safety* **2012**, 11, 378-398.
377   8.   Khan, M. T., Novel tyrosinase inhibitors from natural resources - their computational studies. *Curr*
378   *Med Chem* **2012**, 19, 2262-72.
379   9.   Kim, Y. J.; Uyama, H., Tyrosinase inhibitors from natural and synthetic sources: structure, inhibition
380   mechanism and perspective for the future. *Cell Mol Life Sci* **2005**, 62, 1707-23.
381   10. Seo, S. Y.; Sharma, V. K.; Sharma, N., Mushroom tyrosinase: recent prospects. *J Agric Food Chem* **2003**,
382   51, 2837-53.
383   11. Ubeid, A. A.; Do, S.; Nye, C.; Hantash, B. M., Potent low toxicity inhibition of human melanogenesis
384   by novel indole-containing octapeptides. *Biochim Biophys Acta* **2012**, 1820, 1481-9.
385   12. Solano, F.; Briganti, S.; Picardo, M.; Ghanem, G., Hypopigmenting agents: an updated review on
386   biological, chemical and clinical aspects. *Pigment Cell Res* **2006**, 19, 550-71.
387   13. Halaouli, S.; Asther, M.; Sigoillot, J. C.; Hamdi, M.; Lomascolo, A., Fungal tyrosinases: new prospects
388   in molecular characteristics, bioengineering and biotechnological applications. *J Appl Microbiol* **2006**,
389   100, 219-32.
390   14. Pillaiyar, T.; Manickam, M.; Namasivayam, V., Skin whitening agents: medicinal chemistry
391   perspective of tyrosinase inhibitors. *J Enzyme Inhib Med Chem* **2017**, 32, 403-425.
392   15. Goldfeder, M.; Kanteev, M.; Isaschar-Ovdat, S.; Adir, N.; Fishman, A., Determination of tyrosinase
393   substrate-binding modes reveals mechanistic differences between type-3 copper proteins. *Nat*
394   *Commun* **2014**, 5, 4505.
395   16. Ismaya, W. T.; Rozeboom, H. J.; Weijn, A.; Mes, J. J.; Fusetti, F.; Wichers, H. J.; Dijkstra, B. W., Crystal
396   structure of Agaricus bisporus mushroom tyrosinase: identity of the tetramer subunits and interaction
397   with tropolone. *Biochemistry* **2011**, 50, 5477-86.
398   17. Deri, B.; Kanteev, M.; Goldfeder, M.; Lecina, D.; Guallar, V.; Adir, N.; Fishman, A., The unravelling of
399   the complex pattern of tyrosinase inhibition. *Sci Rep* **2016**, 6, 34993.

400 18.   Klabunde, T.; Eicken, C.; Sacchettini, J. C.; Krebs, B., Crystal structure of a plant catechol oxidase
401   containing a dicopper center. *Nat Struct Biol* **1998**, 5, 1084-90.
402 19.   Choi, J.; Park, S. J.; Jee, J. G., Analogues of ethionamide, a drug used for multidrug-resistant
403   tuberculosis, exhibit potent inhibition of tyrosinase. *Eur J Med Chem* **2015**, 106, 157-66.
404 20.   Choi, J.; Jee, J. G., Repositioning of Thiourea-Containing Drugs as Tyrosinase Inhibitors. *Int J Mol Sci*
405   **2015**, 16, 28534-48.
406 21.   Irwin, J. J.; Shoichet, B. K., Docking Screens for Novel Ligands Conferring New Biology. *J Med Chem*
407   **2016**, 59, 4103-20.
408 22.   Choi, J.; Choi, K. E.; Park, S. J.; Kim, S. Y.; Jee, J. G., Ensemble-Based Virtual Screening Led to the
409   Discovery of New Classes of Potent Tyrosinase Inhibitors. *J Chem Inf Model* **2016**, 56, 354-67.
410 23.   Mysinger, M. M.; Shoichet, B. K., Rapid context-dependent ligand desolvation in molecular docking. *J*
411   *Chem Inf Model* **2010**, 50, 1561-73.
412 24.   Irwin, J. J.; Sterling, T.; Mysinger, M. M.; Bolstad, E. S.; Coleman, R. G., ZINC: a free tool to discover
413   chemistry for biology. *J Chem Inf Model* **2012**, 52, 1757-68.
414 25.   Irwin, J. J., Using ZINC to acquire a virtual screening library. *Curr Protoc Bioinformatics* **2008**, Chapter
415   14, Unit 14 6.
416 26.   Irwin, J. J.; Shoichet, B. K., ZINC--a free database of commercially available compounds for virtual
417   screening. *J Chem Inf Model* **2005**, 45, 177-82.
418 27.   Sato, K.; Toriyama, M., The inhibitory effect of non-steroidal anti-inflammatory drugs (NSAIDs) on
419   the monophenolase and diphenolase activities of mushroom tyrosinase. *Int J Mol Sci* **2011**, 12,
420   3998-4008.
421 28.   Wisansky, W. A.; Martin, G. J.; Ansbacher, S., p-AMINOBENZOIC ACID AND TYROSINASE
422   ACTIVITY. *J Am Chem Soc* **1941**, 63, 1771-1772.
423 29.   McGovern, S. L.; Helfand, B. T.; Feng, B.; Shoichet, B. K., A specific mechanism of nonspecific
424   inhibition. *J Med Chem* **2003**, 46, 4265-72.
425 30.   Dias, A. A.; Pinto, P. A.; Fraga, I.; Bezerra, R. M. F., Diagnosis of Enzyme Inhibition Using Excel Solver:
426   A Combined Dry and Wet Laboratory Exercise. *J Chem Educ* **2014**, 91, 1017-1021.
427 31.   Martin, R. B., Disadvantages of Double Reciprocal Plots. *J Chem Educ* **1997**, 74, 1238.
428 32.   Sun, W.; Wendt, M.; Klebe, G.; Rohm, K. H., On the interpretation of tyrosinase inhibition kinetics. *J*
429   *Enzyme Inhib Med Chem* **2014**, 29, 92-9.
430 33.   Liu, T.; Lin, Y.; Wen, X.; Jorissen, R. N.; Gilson, M. K., BindingDB: a web-accessible database of
431   experimentally determined protein-ligand binding affinities. *Nucleic Acids Res* **2007**, 35, D198-201.
432 34.   Keiser, M. J.; Roth, B. L.; Armbruster, B. N.; Ernsberger, P.; Irwin, J. J.; Shoichet, B. K., Relating protein
433   pharmacology by ligand chemistry. *Nat Biotechnol* **2007**, 25, 197-206.
434 35.   Khatib, S.; Nerya, O.; Musa, R.; Tamir, S.; Peter, T.; Vaya, J., Enhanced substituted resorcinol
435   hydrophobicity augments tyrosinase inhibition potency. *J Med Chem* **2007**, 50, 2676-81.
436 36.   Gaulton, A.; Bellis, L. J.; Bento, A. P.; Chambers, J.; Davies, M.; Hersey, A.; Light, Y.; McGlinchey, S.;
437   Michalovich, D.; Al-Lazikani, B.; Overington, J. P., ChEMBL: a large-scale bioactivity database for
438   drug discovery. *Nucleic Acids Res* **2012**, 40, D1100-7.
439 37.   Aronov, A. M.; McClain, B.; Moody, C. S.; Murcko, M. A., Kinase-likeness and kinase-privileged
440   fragments: toward virtual polypharmacology. *J Med Chem* **2008**, 51, 1214-22.
441 38.   Keough, D. T.; Skinner-Adams, T.; Jones, M. K.; Ng, A. L.; Brereton, I. M.; Guddat, L. W.; de Jersey, J.,
442   Lead compounds for antimalarial chemotherapy: purine base analogs discriminate between human
443   and P. falciparum 6-oxopurine phosphoribosyltransferases. *J Med Chem* **2006**, 49, 7479-86.
444 39.   Hsieh, J. F.; Wu, S. H.; Yang, Y. L.; Choong, K. F.; Chen, S. T., The screening and characterization of
445   6-aminopurine-based xanthine oxidase inhibitors. *Bioorg Med Chem* **2007**, 15, 3450-6.
446 40.   Shea, T. A.; Burburan, P. J.; Matubia, V. N.; Ramcharan, S. S.; Rosario, I., Jr.; Parkin, D. W.; Stockman, B.
447   J., Identification of proton-pump inhibitor drugs that inhibit Trichomonas vaginalis uridine
448   nucleoside ribohydrolase. *Bioorg Med Chem Lett* **2014**, 24, 1080-4.
449 41.   Santana, L.; Gonzalez-Diaz, H.; Quezada, E.; Uriarte, E.; Yanez, M.; Vina, D.; Orallo, F., Quantitative
450   structure-activity relationship and complex network approach to monoamine oxidase A and B
451   inhibitors. *J Med Chem* **2008**, 51, 6740-51.
452 42.   Rohrig, U. F.; Majjigapu, S. R.; Chambon, M.; Bron, S.; Pilotte, L.; Colau, D.; Van den Eynde, B. J.;
453   Turcatti, G.; Vogel, P.; Zoete, V.; Michielin, O., Detailed analysis and follow-up studies of a
454   high-throughput screening for indoleamine 2,3-dioxygenase 1 (IDO1) inhibitors. *Eur J Med Chem* **2014**,
455   84, 284-301.
456 43.   Ma, D. L.; Chan, D. S.; Leung, C. H., Drug repositioning by structure-based virtual screening. *Chem*
457   *Soc Rev* **2013**, 42, 2130-41.

458   44.   Hopkins, A. L.; Keseru, G. M.; Leeson, P. D.; Rees, D. C.; Reynolds, C. H., The role of ligand efficiency
459   metrics in drug discovery. *Nat Rev Drug Discov* **2014**, 13, 105-21.
460   45.   Alijanianzadeh, M.; Saboury, A. A.; Mansuri-Torshizi, H.; Haghbeen, K.; Moosavi-Movahedi, A. A.,
461   The inhibitory effect of some new synthesized xanthates on mushroom tyrosinase activities. *J Enzyme*
462   *Inhib Med Chem* **2007**, 22, 239-46.
463   46.   Irwin, J. J.; Shoichet, B. K.; Mysinger, M. M.; Huang, N.; Colizzi, F.; Wassam, P.; Cao, Y., Automated
464   docking screens: a feasibility study. *J Med Chem* **2009**, 52, 5712-20.
465   47.   Cheng, Y.; Prusoff, W. H., Relationship between the inhibition constant (K1) and the concentration of
466   inhibitor which causes 50 per cent inhibition (I50) of an enzymatic reaction. *Biochem Pharmacol* **1973**,
467   22, 3099-108.
468   48.   Cornish-Bowden, A., *Fundamentals of enzyme kinetics*. John Wiley & Sons: 2013.
469   49.   Motulsky, H. J.; Ransnas, L. A., Fitting curves to data using nonlinear regression: a practical and
470   nonmathematical review. *FASEB J* **1987**, 1, 365-74.
471   50.   Niesen, F. H.; Berglund, H.; Vedadi, M., The use of differential scanning fluorimetry to detect ligand
472   interactions that promote protein stability. *Nat. Protocols* **2007**, 2, 2212-2221.
473   51.   Schrodinger, LLC *The PyMOL Molecular Graphics System, Version 1.3r1*, 2010.